Journal of Muscle Research and Cell Motility **20**: 443–456, 1999.

Measured and modeled properties of mammalian skeletal muscle. I. The effects of post-activation potentiation on the time course and velocity dependencies of force production

IAN E. BROWN[1] and GERALD E. LOEB[2,*]
[1]*Division of Biology 216-76, California Institute of Technology, Pasadena, CA 91125, USA;* [2]*The MRC Group in Sensory-Motor Neuroscience, Department of Physiology, Queen's University, Kingston, ON, Canada, K7L 3N6*

Received 9 June 1998; accepted in revised form 5 April 1999

Abstract

Activation of mammalian fast-twitch skeletal muscle induces a persistent effect known as post-activation potentiation (PAP), classically defined as an increase in force production at sub-maximal levels of activation. The underlying mechanism is thought to be phosphorylation of the myosin regulatory light chain (MRLC), which leads to an increase in the rate constant for cross-bridge attachment (Sweeney *et al.*, 1993). If true, this suggests the hypothesis that other contractile properties should be affected during PAP. Using a feline fast-twitch whole-muscle preparation (caudofemoralis) at 37°C, we observed that PAP greatly increased tetanic forces during active lengthening, decreased isometric tetanic rise times and delayed isometric tetanic force relaxation. The first two of these effects were length dependent with a greater effect occurring at shorter lengths. These findings confirmed that PAP has other functionally important effects beyond a simple increase in sub-maximal isometric forces. Furthermore, length was found to have an effect independent of PAP on the shortening half of the FV relationship (less force was produced at longer lengths) and on the rate of force relaxation during the later stages of isometric tetanic force decay (slower relaxation at longer lengths). All of these findings can be explained with a simplified, two-state model of cross-bridge dynamics that accounts for the interaction of both interfilament spacing and MRLC phosphorylation on the apparent rate constants for cross-bridge attachment and detachment. These findings are largely consistent with data collected previously from reduced preparations such as skinned fibers at cold, unphysiological temperatures (e.g. 5°C). One finding that could not be explained by our model was that twitch fall times in the dispotentiated state were parabolically correlated with length, whereas in the potentiated state the relationship was linear. The time course of decay of this effect did not follow the time course of force dispotentiation, suggesting that there are other activation-dependent processes occurring in parallel with MRLC phosphorylation.

Introduction

Attempts to model force production in mammalian skeletal muscle under physiological conditions have been hampered by a lack of appropriate data. One such condition that has been largely ignored is post-activation potentiation (PAP), commonly defined as an increase or potentiation of force at sub-maximal stimulus frequencies following recent azctivity in fast-twitch muscle (see Sweeney *et al.*, 1993, for review). Although much work has focused on the effects of PAP in relation to peak isometric twitch forces (e.g. Close and Hoh, 1968; Moore and Stull, 1984; Brown and Loeb, 1998), little is known about its effects on other contractile properties. Recently (Brown and Loeb, 1998) we concluded that fast-twitch muscles seem likely to spend much, if not most of their activated life in the potentiated state. They only enter a state we call 'dispotentiation' after long periods of disuse or inactivity. It follows logically from this conclusion that we must characterize the contractile properties of fast-twitch muscle in both the potentiated and dispotentiated states in order to build an accurate, physiologically relevant model of muscle force production.

The mechanism that is thought to be primarily responsible for PAP is phosphorylation of the myosin regulatory light chain (MRLC, see Sweeney *et al.*, 1993, for review). Phosphorylation of MRLC has been shown to increase the rate constant for cross-bridge attachment thereby resulting in twitch force potentiation (Metzger *et al.*, 1989; Sweeney and Stull, 1990). If true, it seems likely that PAP should also affect other contractile properties of muscle.

Because there already exists a good understanding of how PAP affects peak isometric twitch and tetanic forces (Close and Hoh, 1968; Moore and Stull, 1984; Brown and Loeb, 1998), the primary focus of the present study

*To whom correspondence should be addressed, *Current address:* Department of Biomedical Engineering, University of Southern California, Los Angeles, CA 90089; E-mail: GLoeb@BMSRS.USC.edu; Tel.: 213-821-1112

was to examine and characterize how PAP affected other contractile properties, including the tetanic FV relationship and twitch and tetanic rise and fall times. Previous studies that examined the effects of PAP on twitch fall times have been contradictory, with some studies suggesting that PAP increases twitch fall time (Botterman *et al*., 1986) while others suggest that PAP decreases twitch fall time (Close and Hoh, 1968; Vandenboom and Houston, 1996). Previous work on the tetanic FV relationship has suggested that PAP has little effect on the FV relationship (Grange *et al*., 1995), but only shortening velocities were tested in that study. Our intent was therefore to clarify and extend these earlier studies. An additional consideration that went into the design of our experiments was to look for possible interactions between PAP and length, based upon recent evidence that the effects of PAP are greater at shorter lengths (Brown and Loeb, 1998; Yang *et al*., 1998).

A secondary purpose of this study was to use the data collected for our model to test current hypotheses of the mechanisms of muscle contraction and potentiation. Much of the evidence that has been used in the past to probe these basic mechanisms has been collected under highly artificial, albeit well-controlled conditions, for example single skinned muscle fiber preparations at unphysiologically low temperatures (Brenner, 1983; 1988; Metzger *et al*., 1989; Sweeney and Stull, 1990; Higuchi and Goldman, 1995). While such preparations have been useful to develop mechanistic hypotheses of muscle contraction, it is important to extend this previous work to physiologically relevant preparations. In particular, how well can a simplified two-state Huxley-style model of cross-bridge dynamics based upon previous single fiber work at low temperatures explain our findings in electrically active whole muscle at normal body temperature?

In continuation of a previous study (Brown and Loeb, 1998), we performed these experiments in feline caudofemoralis (CF), an exclusively fast-twitch hip extensor/abductor. CF is ideal for whole-muscle experiments (Brown *et al*., 1998) because of its fiber composition, its simple architecture and its high ratio of fascicle length to aponeurosis length (ca. 5:1), which results in a whole-muscle preparation with very little in-series compliance. CF has a mean fascicle length of 5–6 cm and can produce 15–20 N force under isometric, tetanic conditions (Brown *et al*., 1998). A preliminary account of these findings has been published (Brown and Loeb, 1997).

Materials and methods

The experimental apparatus and procedures used in this study are similar to those used and described previously for feline CF muscle (Brown and Loeb, 1998). All experiments were carried out in 13 cats of either sex (2.4–5.1 kg) under deep pentobarbital anesthesia as determined by the absence of pedal withdrawal. Briefly, the feline CF muscle was studied *in vivo*, dissected free of surrounding tissue with its origin, innervation and blood supply left intact and maintained thermostatically at $37 \pm 1°C$ in a mineral oil pool. The length of the muscle fascicles was controlled by clamping onto caudal vertebrae Ca2 and Ca3 (CF origin) and onto the insertion tendon just at the point where the distal-most fibers terminate, eliminating virtually all series-compliance in the linkage. The insertion clamp was attached to a computer-controlled muscle puller via a force transducer. Electrical stimulation was applied via platinum-iridium hook electrodes on cut L7 and S1 ventral roots and monitored by recording M-waves via two multi-stranded stainless steel wire electrodes inserted transversely through the muscle ca. 5 mm apart. Computer templates controlled the length and stimulus patterns simultaneously for long preprogrammed sequences defining entire experimental protocols in 1.667 ms steps. During each step, the computer program recorded values for both the force and a rectified, bin-integrated representation of the M-waves. Force was digitally filtered after the experiment using a double-pass, second-order Butterworth filter with a 3 dB cutoff frequency of 120 Hz to remove high-frequency (150–200 Hz) resonant noise from our system.

At the beginning of each experiment passive and tetanic FL curves were collected in the dispotentiated state (as described below). Passive force data were collected in the isometric state 30 ms after stretching to at least 15 different lengths. These passive forces were then subtracted post-experiment from all subsequent force records to provide an estimate of active force. Preliminary estimation of L_0 for the tetanic FL curves was made based upon *in situ* anatomical lengths (Brown *et al*., 1998). Based on this estimate, isometric tetanic contractions (120 pps, 15 p trains) were elicited at 0.7, 0.8, 0.9, 0.95, 1.0, 1.05, 1.1 and 1.2 L_0. The 'true' L_0 was then chosen as the length at which maximal tetanic isometric force (F_0) could be elicited. Sarcomere length measurements were not collected during these experiments because previous work with CF has demonstrated that the peak of the tetanic FL relationship occurs reliably at ca. 2.5 μm, as expected based upon sliding filament theory (Brown *et al*., 1998).

Two basic protocols of stimulation were used in this study to produce two different states of muscle: dispotentiated and potentiated. Data in the dispotentiated state were collected prior to data in the potentiated state unless otherwise noted. For the dispotentiated protocols, all stimuli were separated by 5 min intervals to avoid potentiation (Brown and Loeb, 1998). The potentiated protocols used stimulus trains always separated by 7 s. Potentiation was achieved by applying twelve isometric 10 p trains at 60 pps at three successive lengths (0.75, 0.95 and 1.15 L_0) and maintained with 30 pps–120 pps stimulus trains (10 p–12 p duration). This protocol has been shown previously to provide a stable and apparently maximal level of potentiation in CF without significant fatigue (Brown and Loeb, 1998). The muscle and nerve preparations were allowed to

equilibrate for 45–60 min prior to and between each stimulus protocol. In all paradigms stimulation voltage (0.2 ms rectangular pulses) was five times higher than the threshold required to elicit an M-wave. M-wave amplitude was monitored continuously to ensure complete activation of the entire muscle throughout the experiment. We inserted single isometric twitches at 1.0 L_0 one second before specified experimental trains so that peak twitch force could be used as a measure of potentiation (Brown and Loeb, 1998).

Results

As described in Materials and methods, passive forces (not shown) were subtracted from recorded force to provide an estimate of active force. Passive forces were minimal (less than 3% of F_0) at the longest lengths tested for all of the tetanic data, but did reach substantial values at the longest lengths tested during the twitch data collection (up to 0.35 F_0). Records of electromyogram activity, which were recorded in every experiment under all conditions, are also not shown because activation history had no apparent effect on them.

Tetanic force-velocity relationships

Tetanic force-velocity (FV) relationships were constructed using data from isovelocity trials. Force data were collected at the end of tetanic stimulus trains (120 pps, 15 p stimuli) for a range of positive and negative velocities from three animals. Data were collected during four different conditions: in both the potentiated and dispotentiated states at each of two different lengths (0.8 and 1.1 L_0). To avoid damage from active lengthening (Brown and Loeb, 1995), fast stretches were not applied at 1.1 L_0. In one of the animals the potentiated data were collected prior to dispotentiated data, with no obvious differences in the results. Sample force and length traces collected at 0.8 L_0 in the potentiated state are shown in Figure 1A with the accompanying FV relationship in Figure 1B. As expected, active shortening produced less force than isometric whereas active lengthening produced greater force.

Mean FV data from all three animals in all four conditions are shown in Figure 2A and 2B, plotted so as to examine the effects of potentiation at each of the two lengths. All force data were first normalized to isometric to remove the effects of filament overlap. The effects of potentiation were similar at both short and long lengths. Potentiation had little effect on force during active shortening; only at shorter muscle lengths and at slow shortening velocities was there a small but statistically significant effect: potentiation resulted in a *smaller* normalized force. In contrast, potentiated muscle produced significantly larger forces than dispotentiated muscle during active lengthening. The FV slope around isometric appeared to be continuous for CF in all four states (slopes around isometric estimated from data points at $\pm 0.1 L_0$/s compared to isometric; all four paired t-tests produced $P > 0.05$).

The fast-twitch data from Figure 2A and 2B were replotted in Figure 2C and 2D so as to examine more closely the effects of length on the FV relationship in each of the dispotentiated and potentiated states. In the dispotentiated state, length appears to affect the entire FV relationship; longer lengths produce relatively smaller forces during shortening and relatively greater forces during lengthening. In contrast, length appears to affect only the shortening half of the FV curve in the potentiated state with longer lengths producing relatively smaller forces, although the lack of data at faster lengthening velocities precludes a more general conclusion.

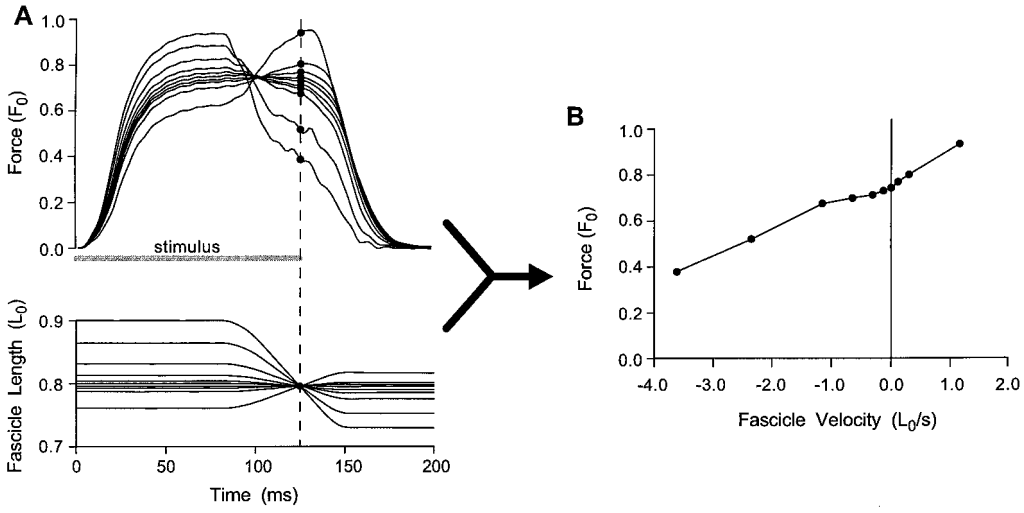

Fig. 1. Sample tetanic FV data. **A**. Sample force and length traces from a potentiated muscle stimulated for 15 p at 120 pps. Shaded bar indicates duration of stimulus. Tetanic FV data were collected at the end of stimulus trains (dashed line) as indicated by the dots and used to construct a FV relationship as shown in **B**.

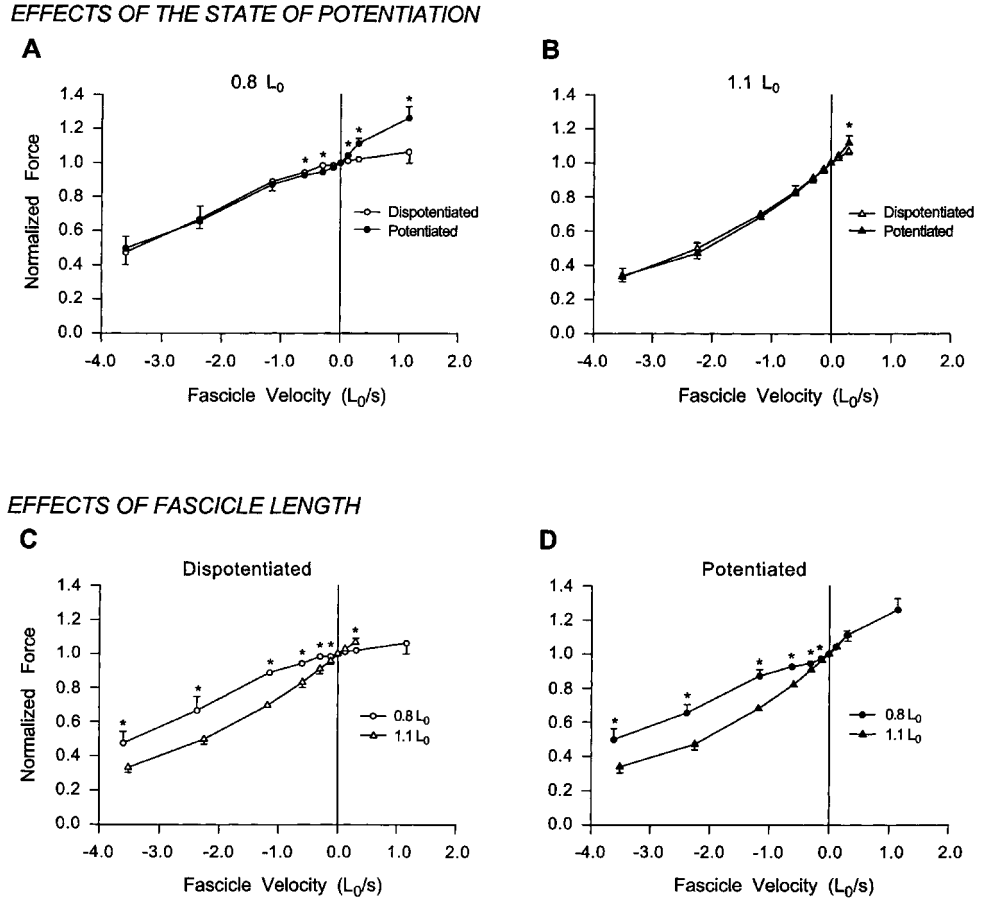

Fig. 2. Mean FV data. FV relationships were constructed as shown in Figure 1, but with all forces normalized to isometric force. Error bars indicate SD about the mean ($N = 3$, SD not shown if less than 0.02). **A**, **B**. Comparison of FV data collected in dispotentiated state (open symbols) vs. potentiated state (filled symbols). **A** and **B** show data collected at 0.8 and 1.1 L_0 respectively. * indicates a significant difference between potentiated and dispotentiated states ($P < 0.05$, paired t-test). **C**, **D**. Comparison of FV relationships collected at 0.8 L_0 (circles) vs. 1.1 L_0 (triangles). **C** and **D** show data collected in dispotentiated and potentiated states respectively. These data are the same data as plotted in **A** and **B**. * indicates a significant difference between 0.8 and 1.1 L_0 ($P < 0.05$, paired t-test).

Tetanic rise and fall times

Isometric tetanic contractions were elicited at fascicle lengths ranging from 0.8–1.1 L_0 in 10 animals in both the dispotentiated and potentiated states (the anatomical range of motion of CF is ca. 0.6–1.2 L_0; functional range during walking has been estimated as ca. 0.95–1.15 L_0; Brown *et al.*, 1998). Sample force traces at 0.8 and 1.1 L_0 are shown in Figure 3A and 3B. As has been noted previously, peak potentiated forces tend to be somewhat lower than peak dispotentiated forces, possibly due to some sort of short-term fatigue (Brown and Loeb, 1998). Force developed more quickly and decayed more slowly in the potentiated state at both short and long lengths. While the effect of potentiation on force decay was similar at both lengths, the effect of potentiation on force development was length dependent; potentiation produced a greater effect at shorter lengths.

Various measures of rise and fall times were collected from the force traces of all ten animals and the means (±SD) of the potentiated state, dispotentiated state and the difference between those states were plotted versus length (Figure 4A–4D). For half rise times (t_{0-50}) the dispotentiated and difference data were correlated linearly to length ($r > 0.66$, $P < 0.01$) where as the potentiated data were uncorrelated ($r < 0.15$, $P > 0.1$). For t_{20-80} rise times the potentiated and difference data were correlated linearly to length ($r > 0.52$, $P < 0.02$) whereas the dispotentiated data were uncorrelated ($r < 0.06$, $P > 0.1$). For both measures of fall time (t_{100-50}; t_{80-20}) the potentiated and dispotentiated data were correlated linearly to length ($r > 0.52$, $P < 0.02$) whereas the difference data were uncorrelated ($r < 0.21$, $P > 0.1$). The mean (±SD) differences for the fall times (-9.9 ± 6.0 ms and -2.0 ± 3.9 ms respectively) were both statistically different from zero ($t = -7.42$, $P < 0.001$; $t = -2.31$, $P < 0.05$ respectively), but the large variability observed between animals in the t_{80-20} difference data suggests that this difference may not be meaningfully different from zero.

Twitch rise and fall times

Isometric twitches at lengths ranging from 0.8–1.35 L_0 were collected in five animals in both the potentiated

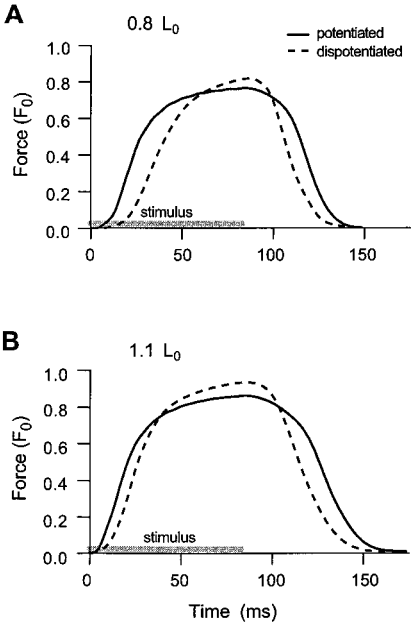

Fig. 3. Sample tetanic isometric data. **A**, **B**. Sample isometric tetanic force traces at 0.8 and 1.1 L_0 respectively from a muscle stimulated for 10 p at 120 pps. Data were collected from both dispotentiated muscle (dashed lines) and potentiated muscle (solid lines). Shaded bar indicates duration of stimulus. At both lengths force production began earlier and ended later in the potentiated state. The difference in time course between dispotentiated and potentiated states was similar for the two lengths during the falling phase of force but was greater at short lengths during the rising phase.

and dispotentiated states (same data set as reported previously by Brown and Loeb, 1998). Force profiles of the twitches from one experiment are shown in Figure 5A and 5B. In both the dispotentiated and potentiated states both rise and fall times appear to increase as length is increased. Twitches were, in general, shorter in duration in the potentiated state than in the dispotentiated state. As described previously by Brown and Loeb (1998) the amount of potentiation observed for peak twitch forces was highly length dependent, ranging from ca. 400% increase in peak twitch force at 1.0 L_0 to $<60\%$ increase at lengths greater than 1.3 L_0.

Various measures of twitch rise time ($t_{0\text{–}100}$; $t_{20\text{–}80}$) and fall time ($t_{100\text{–}50}$; $t_{80\text{–}20}$) were averaged from all five animals and examined for interactions between potentiation and length. The results of these measures are plotted in Figure 6A–6D. Both measures of rise time ($t_{0\text{–}100}$ and $t_{20\text{–}80}$) were correlated linearly with fascicle length in both the potentiated and dispotentiated states, as was the difference between the two states ($r > 0.32$, $P < 0.01$). Both measures of fall time ($t_{100\text{–}50}$; $t_{80\text{–}20}$) were correlated linearly with length ($r > 0.94$, $P < 0.001$) in the potentiated state and correlated parabolically with length in the dispotentiated state ($r > 0.93$, $P < 0.001$); the difference between the two states was also correlated parabolically with length ($r > 0.88$, $P < 0.001$).

As will become clear in the discussion, the hypothesized effects of MRLC phosphorylation could not explain readily the changes in twitch fall time associated with potentiation. To test the hypothesis that MRLC phosphorylation might not be responsible for the changes in twitch fall time associated with recent activation, we recorded the time course of changing isometric twitch fall times ($t_{80\text{–}20}$ at 1.3 L_0) and plotted them against the time course of dispotentiation (as measured by the peak force of an isometric twitch at 1.0 L_0) for four animals. As can be seen in Figure 7 the time courses of these two phenomena are clearly different ($r = 0.09$ over the first 300 s; $P > 0.1$). Furthermore, the potentiation of force was robust and consistent among preparations whereas the change in twitch relaxation varied considerably.

Discussion

The data presented here provide new evidence about the functional importance of PAP. Previously it was thought that the primary effect of PAP was a simple increase in force output at sub-maximal levels of activation. We have shown here that PAP also increases significantly the slope of the FV relationship around isometric, and is accompanied by large increases in force during active lengthening. Modeling studies have demonstrated that under certain conditions the slope of the FV relationship around isometric can dominate muscle behavior (Brown and Loeb, 1999). Coupled with recent evidence that the normal operating state of fast-twitch muscle is the potentiated state (Brown and Loeb, 1998), we speculate that this second effect might be another functionally important consequence of PAP.

These data also provide much corroborating evidence in support of current theories of muscle contraction. Much of the data used to build current theories of muscle contraction have been collected from highly reduced preparations such as single, skinned muscle fibers at low, unphysiological temperatures. Here, we extend that work to include a description of the contractile properties of muscle in a more physiologically relevant preparation. Excitation of the whole muscle via an intact neuromuscular and calcium release system provides additional data about the dynamics of activation of the contractile apparatus that can be used to extend and test such theories. As described below, we believe that the changes we observed in the FV relationship and tetanic rise times are caused by the same mechanism responsible for PAP-phosphorylation of the myosin regulatory light chain (MRLC). The mechanism responsible for the changes in twitch fall time is as yet unidentified.

PAP-related phenomena

The following discussion assumes that PAP in feline CF is accompanied by an increase in MRLC phosphorylation, as has been shown previously for rat (Moore and Stull, 1984), rabbit (Moore *et al.*, 1985), mouse (Grange

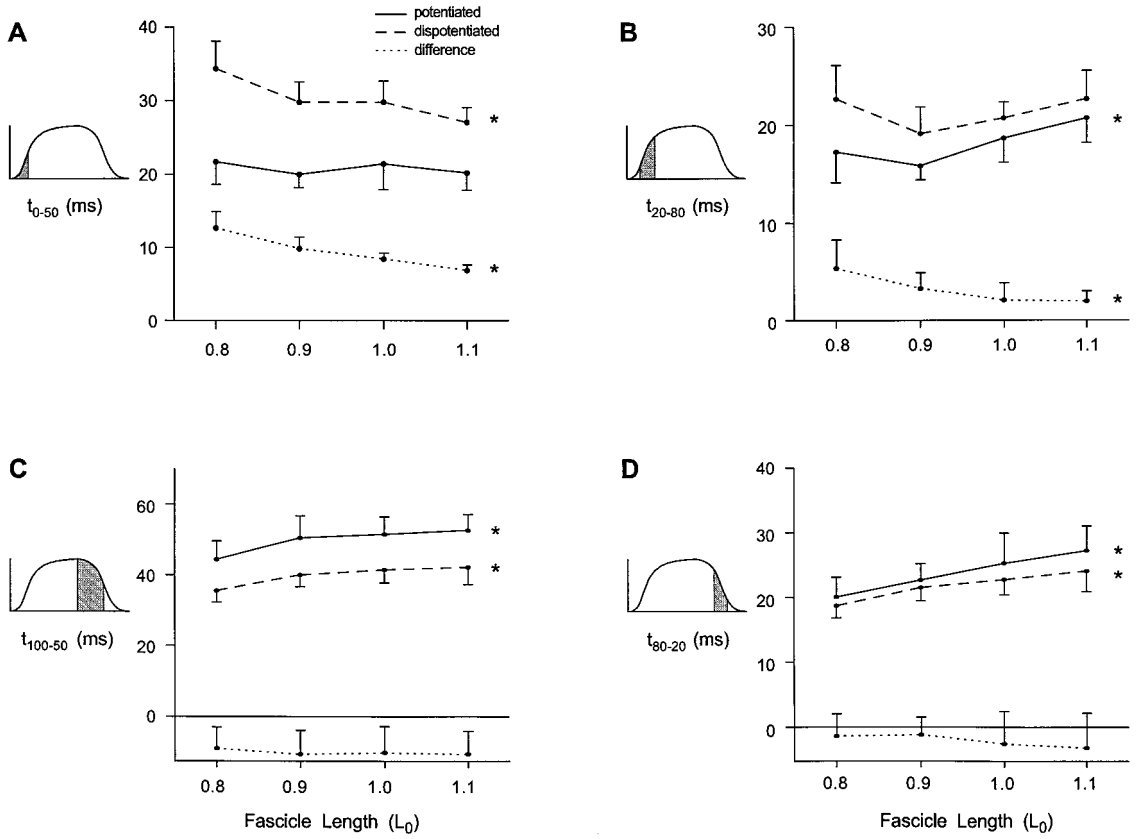

Fig. 4. Mean tetanic isometric rise and fall times. Various measures of rise and fall times were collected from a total of ten animals at four lengths. Tetanic stimulus trains were at 120 pps for 10–15 p. Sample force records are shown in Figure 3. $t_{m\text{–}n}$ refers to the time from m% to n% of peak force as shown pictorially in the y-axis label of each graph. Mean (±SD) data were plotted for the potentiated state (solid lines), the dispotentiated state (dashed lines) and the difference between states (dotted lines). N ranged from 4–6 at each length. * beside a data set indicates that it was correlated linearly with length ($P < 0.02$).

et al., 1995), human (Houston and Grange, 1990) and even for non-mammalian species such as frog (Morano *et al.*, 1988). This assumption is based upon the ubiquitous nature of this phenomenon as well as the identical effects of PAP observed thus far in CF as compared to those observed in other species including: (1) a ca. 60% increase in peak isometric twitch force following potentiation at the fascicle length producing peak isometric twitch force (Brown and Loeb, 1998), similar to values reported previously for other feline muscles (Burke *et al.*, 1976) as well as rat (Krarup, 1981; Moore and Stull, 1984; MacIntosh and Gardiner, 1987), mouse (Moore *et al.*, 1990), rabbit (Moore *et al.*, 1985) and frog (Close, 1972); (2) interactions between length and isometric twitch potentiation in which greater potentiation is observed at shorter lengths (Brown and Loeb, 1998), similar to reports in frog (Close, 1972) and similar to the effects of MRLC phosphorylation on calcium-induced force production in skinned rabbit fibers (Yang et al., 1998); (3) the time course of development and decay of PAP (Brown and Loeb, 1998), similar to the time course of MRLC phosphorylation and dephosphorylation in rat (Moore and Stull, 1984; Stull *et al.*, 1990); (4) the minimal effect of PAP on the shortening half of the FV curve (discussed below), similar to effects seen in man (Stuart *et al.*, 1988) and mouse (Grange *et al.*, 1995) and similar to reports in rabbit fibers following MRLC phosphorylation (Persechini *et al.*, 1985); and (5) the complex effects of recent activity and length on the rise and fall times of twitches (discussed below), similar to other feline muscles (Botterman *et al.*, 1986) as well as rat (Close and Hoh, 1968; Woittiez *et al.*, 1984), mouse (Vandenboom and Houston, 1996) and frog (Hartree and Hill, 1921; Close, 1972). All of these phenomena except for the effects on twitch fall time can be explained by a logically simple model of cross-bridge kinetics as developed below. This Huxley-style model describes the effects of length, velocity and potentiation upon individual cross-bridge force production and how these effects sum together when an entire population of cross-bridges is considered.

Myofilament and cross-bridge model

Active force is a complex function of sarcomere length, velocity, activation history, state of potentiation and fatigue. The best-understood of these factors is the classical FL relationship based on myofilament overlap and the number of cross-bridges formed. It is well known, however, that after removing this effect from a set of experimental data, there remain substantial interactions between sarcomere length and the other

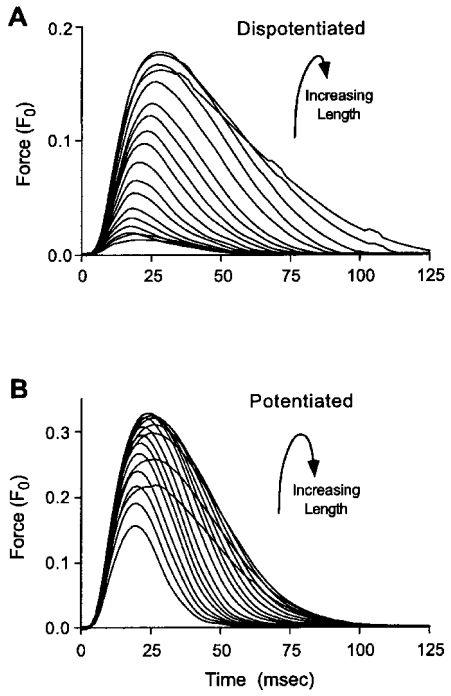

Fig. 5. Sample isometric twitch data. **A**, **B**. Sample force traces of isometric twitches in the dispotentiated and potentiated states (note the different force scales). Fascicle lengths ranged from 0.8–1.35 L_0. Both rise and fall time appeared to increase with length. Potentiated twitches tended to be shorter in duration than the corresponding dispotentiated twitches.

determinants of active force (Stephenson and Wendt, 1984). Sarcomere length has another geometrical effect on the contractile apparatus, namely changes in the myofilament lattice spacing. In the following analysis, we attempt to account for the remaining interactions with length on the basis of hypothetical interactions between lattice spacing and the rate constants for attachment and detachment of cross-bridges. Many of the ideas used in this discussion were first set forth by Huxley (1957) and Hill (1974).

As suggested by Brenner (1988) and Sweeney and Stull (1990), let us collapse the many states of the cross-bridge cycle into two states: attached (force-producing) and detached (non-force producing). The apparent rate constants for attachment and detachment are then defined as f_{app} and g_{app} respectively, where for simplicity we define g_{app} to include also forcible detachment (i.e. cross-bridge detachment without ATP hydrolysis) as is thought to occur during active lengthening. Cross-bridges are assumed to act independently. A pictorial representation of an attached cross-bridge is shown in Figure 8A. The cross-bridge is assumed to rotate about a pivot producing an angle (θ) between itself and the thin filament. This representation is provided only to illustrate our explanation; its specific form is not critical to our hypotheses.

Within this model framework, f_{app} and g_{app} must vary with cross-bridge angle in a manner qualitatively similar

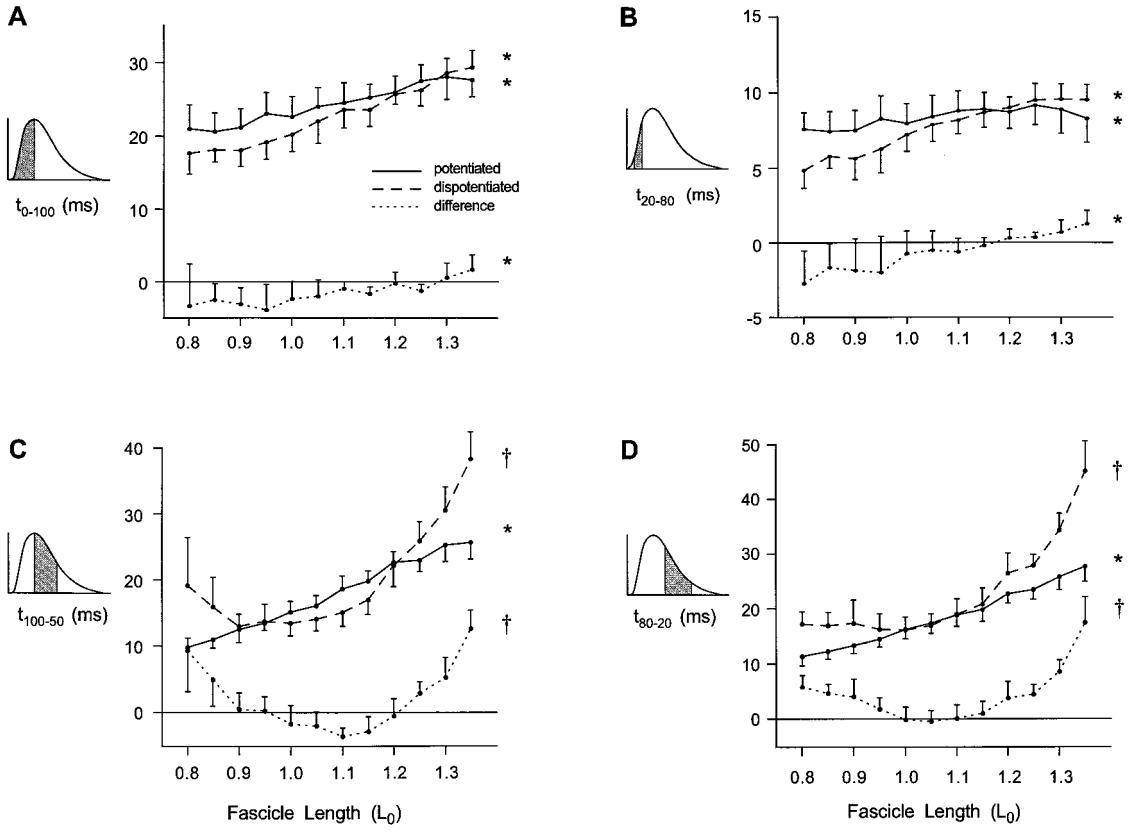

Fig. 6. Mean isometric twitch rise and fall times. Various measures of rise and fall times were collected from five experiments. Sample force records are shown in Figure 5. $t_{m\text{–}n}$ refers to the time from m% to n% of peak force as shown pictorially in the y-axis label of each graph. The mean (±SD) times were plotted vs. fascicle length to compare between the potentiated state (solid lines), the dispotentiated state (dashed lines) and the difference between the states (dotted lines). All data sets were either linearly (*) or parabolically (†) correlated with length ($P < 0.01$).

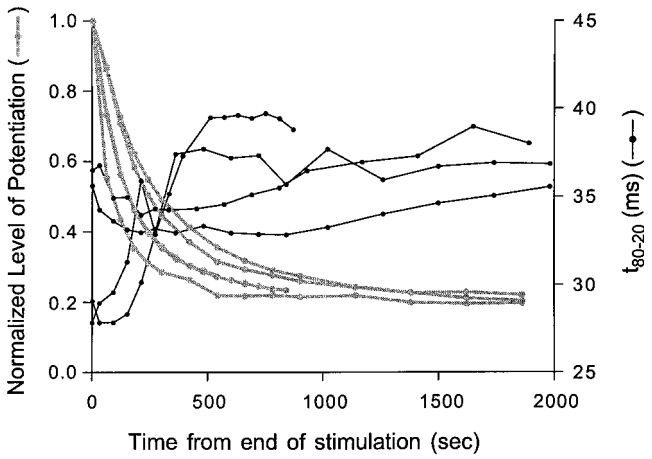

Fig. 7. Time course of changing isometric twitch fall times (t_{80-20}) compared to the time course of dispotentiation. Muscles were potentiated (as described in Materials and methods) and then allowed to dispotentiate. Data from each of four experiments are plotted, starting at the end of stimulation. The normalized level of potentiation was measured by using the peak force of isometric twitches at 1.0 L_0 (thick gray lines) whereas the time course of changing twitch fall times was examined using isometric twitches at lengths ranging from 1.3–1.35 L_0 (thin black lines). Twitches at the two fascicle lengths were applied alternately every 30 or 60 s. The time courses of these two phenomena were uncorrelated over the first 300 s ($r = 0.09$; $P > 0.1$).

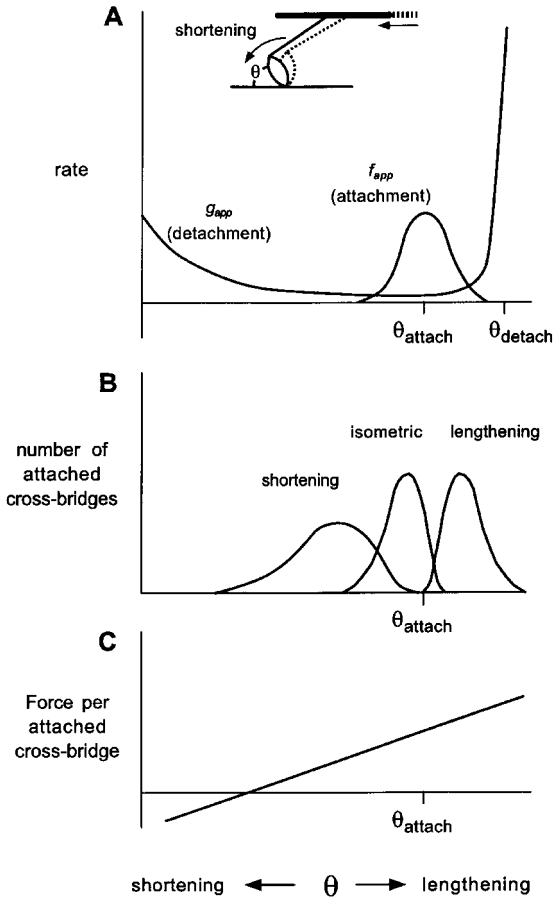

Fig. 8. Schematic description of a two-state cross-bridge model. **A**. Qualitative description of the manner in which the apparent rate constants for cross-bridge attachment (f_{app}) and detachment (g_{app}) vary with the angle between the myosin head and the thin filament (θ). Inset figure shows a schematic of the cross-bridge; as a muscle is allowed to shorten the myosin head rotates and θ decreases. In our model we define $g_{app}(\theta)$ to include also forcible detachment (i.e. cross-bridge detachment without ATP hydrolysis) as is thought to occur during active lengthening. The rate function $f_{app}(\theta)$ is maximal at some attachment angle (θ_{attach}), decreasing at either larger or smaller angles. The rate function $g_{app}(\theta)$ is minimal at some other angle (not marked), increases relatively slowly at θ less then θ_{attach} and increases dramatically at θ greater then θ_{attach}, asymptoting at the detachment angle θ_{detach}. This detachment angle corresponds to the critical extension required to break attached cross-bridges (estimated at 10–15 nm; Lombardi and Piazzesi, 1990; Steinen *et al.*, 1992). **B**. Qualitative description of the relative distributions of attached cross-bridges during shortening, isometric and lengthening conditions. During shortening the distribution skews to smaller angles whereas during lengthening the distribution is forced to angles greater than the attachment angle. **C**. Qualitative description of the relationship between cross-bridge force and θ. Although this is shown as a linear relationship, we need only assume that cross-bridge force increases monotonically with θ as described in text.

to that shown in Figure 8A. There must be some nominal attachment θ or range of θ for which the rate function $f_{app}(\theta)$ is maximal and some θ or range of θ for which the rate function $g_{app}(\theta)$ is minimal. These values need not be identical. We can further identify a cross-bridge detachment angle that corresponds to the critical half-sarcomere extension required to 'break' attached cross-bridges during stretch (estimated at 10–15 nm; Lombardi and Piazzesi, 1990; Steinen *et al.*, 1992). The rate function for detachment, $g_{app}(\theta)$, must rise dramatically at this critical extension to account for these findings as shown in Figure 8A. We remind the reader here again that in our model $g_{app}(\theta)$ includes non-ATP-hydrolyzing forcible detachment as is thought to occur during active lengthening. Complementary evidence for detachment during shortening has been far more difficult to obtain. Recently, Higuchi and Goldman (1995) showed that the working stroke length for a cross-bridge (shortening distance associated with the hydrolysis of a single ATP molecule) during high-speed shortening can reach 60 nm and perhaps much larger. Because the estimated physical stroke length for a single attached cross-bridge is closer to 10–20 nm (Higuchi and Goldman, 1995), this finding implies that a single cross-bridge must interact with several actin binding sites during a single working stroke, temporarily detaching and re-attaching. In the context of our model, all these temporary states are included as part of our force-producing attached state (thus our 'attached' state paradoxically includes some intermediate detached states). In terms of our model, Higuchi and Goldman's findings mean that at high shortening speeds a cross-bridge can remain in the 'attached' state approximately five times as long as during a stretch of equivalent speed (>60 nm during shortening versus 10–15 nm during stretch). The apparent rate constant for detachment in our model must then be approximately five times smaller during shortening as compared to during lengthening. This result is shown qualitatively in Figure 8A.

The manner in which the rate functions $f_{app}(\theta)$ and $g_{app}(\theta)$ vary with θ determines the distribution of

attached cross-bridges. During steady-state isometric conditions, the distribution should be qualitatively similar to that shown in Figure 8B. Cross-bridges will attach near the attachment angle; because there is no motion, none of the individual cross-bridge angles will change. If a sarcomere then begins to shorten, cross-bridge heads will rotate and θ for each attached cross-bridge will become smaller, skewing the distribution to smaller θ. As cross-bridges complete their cycle and detach at various angles of θ, they will re-attach back near the attachment angle. The steady-state distribution of attached cross-bridges during shortening will thus become skewed towards angles smaller than the attachment angle (Figure 8B). The converse situation will occur during active lengthening. As a sarcomere is stretched from isometric, cross-bridge heads will rotate and individual cross-bridge angles will become greater. Once again, as cross-bridge angles change, individual cross-bridges will detach and then re-attach back near the attachment angle. The distribution of attached cross-bridges during steady-state active lengthening will thus become skewed towards angles larger than the attachment angle.

How do these changes in cross-bridge distribution affect force? Huxley (1957) assumed originally that there was a linear relationship between force and cross-bridge extension (or in our model, cross-bridge angle). Recent experiments (Julian and Sollins, 1975; Goldman *et al.*, 1988) have provided evidence that this is, in fact, a reasonable approximation. (For the purposes of our model, we need only assume that force per cross-bridge increases monotonically with θ (Figure 8C), a necessary property to account for short-range stiffness.) During active lengthening, as the distribution of attached cross-bridges skews to larger angles, the net force from all attached cross-bridges will increase because individual cross-bridges will be providing more force. The opposite situation will occur during active shortening. As cross-bridge angles decrease during shortening each attached cross-bridge produces less and less force, and at some angle they even begin to produce negative force (i.e. they begin to oppose shortening). At maximum shortening velocity, the negative forces from some cross-bridges balance the positive forces from others to produce zero net contractile force. Force per cross-bridge appears to be independent of both MRLC phosphorylation (Metzger *et al.*, 1989; Sweeney and Stull, 1990) as well as sarcomere length (Gordon *et al.*, 1966; Civan and Podolsky, 1966; Huxley and Simmons, 1973), which enables the following logical arguments.

Let us introduce two new terms, $\overline{f_{app}}$ and $\overline{g_{app}}$, to represent the apparent rate constants for attachment and detachment for the *population of cross-bridges* as a whole. To calculate these terms (using $\overline{g_{app}}$ as an example), g_{app} for each cross-bridge needs to be determined using that cross-bridge's θ and the rate function $g_{app}(\theta)$. $\overline{g_{app}}$ is calculated as the mean g_{app} for all attached cross-bridges. Therefore $\overline{f_{app}}$ and $\overline{g_{app}}$ depend not only upon the rate functions $f_{app}(\theta)$ and $g_{app}(\theta)$, but also upon the distribution (as a function of θ) of detached and attached cross-bridges, which in turn may depend upon velocity. In the steady-state condition, the fraction of attached cross-bridges (a_{SS}) is determined by the following relationship (Sweeney and Stull, 1990):

$$a_{SS} = \frac{\overline{f_{app}}}{\overline{f_{app}} + \overline{g_{app}}} \quad (1)$$

For the condition of maximal, isometric activation $\overline{f_{app}}$ has been shown to be much greater than $\overline{g_{app}}$ (Sweeney and Stull, 1990). This implies that almost 100% of all cross-bridges are attached and that small changes in either $\overline{f_{app}}$ or $\overline{g_{app}}$ will have little effect upon the fraction of attached cross-bridges under such conditions.

Effects of MRLC phosphorylation

Many of the studies that have looked for an effect of phosphorylation of the myosin regulatory light chain (MRLC) have used skinned single fibers. With such a preparation, it has been shown that MRLC phosphorylation produces a reversible shift in the force-pCa relationship to lower concentrations of calcium, indicating an increase in the sensitivity of the contractile machinery to calcium (reviewed by Sweeney *et al.*, 1993) without an increase in the myosin ATPase rate (Sweeney and Stull, 1990). Using a similar two-state model of cross-bridge kinetics to that described above, Sweeney and Stull (1990) demonstrated that the effects of MRLC phosphorylation occur via changes in cross-bridge attachment (i.e. $\overline{f_{app}}$), and not through changes in detachment (i.e. $\overline{g_{app}}$). The cause of this effect has been postulated to be a reduction in the mean distance between the myosin head and actin, which has been shown to occur following MRLC phosphorylation (Levine *et al.*, 1996).

If the above postulate is true, then changes in interfilament spacing, which would also reduce the mean distance between the myosin head and actin, should also affect $\overline{f_{app}}$ and hence produce an effect analogous to MRLC phosphorylation. Indeed, increases in sarcomere length, which reduce interfilament spacing (Huxley, 1953; Elliott *et al.*, 1963), also shift the force-pCa relationship to lower levels of calcium (Moisescu and Thieleczek, 1979; Stephenson and Williams, 1982; Moss *et al.*, 1983) as do decreases in interfilament spacing caused by osmotic compression (Godt and Maughan, 1981; Martyn and Gordon, 1988; Yang *et al.*, 1998; however, see Moisescu and Thieleczek, 1979). Furthermore, if MRLC phosphorylation and changes in interfilament spacing produce their effect via similar mechanisms (i.e. reducing the mean distance between actin and myosin) then their effects should be interdependent. Yang *et al.* (1998) recently demonstrated this interdependence in isometric single skinned rabbit fibers, by showing that the effects of MRLC phosphorylation on the force-pCa relationship are large at shorter lengths and low osmotic pressures (i.e. large interfilament

spacing) but disappear at either long lengths or high osmotic pressures (i.e. small interfilament spacing). In the following analysis, we consider separately the analogous effects in CF during active lengthening and active shortening.

Active Lengthening

After accounting for filament overlap effects, we observed that both potentiation and length affected tetanic force during active lengthening in an interdependent manner. Yang *et al.* (1998) have shown that the effects of MRLC phosphorylation and length on sub-maximal, isometric force are also interdependent. A summary comparison of the results from these two studies (Table 1, first two columns) shows a striking similarity between the effects of potentiation (or MRLC phosphorylation) and length for these two very different conditions, supporting our central hypothesis that they are all due to changes in $\overline{f_{app}}$.

For changes in $\overline{f_{app}}$ to affect force, the fraction of attached cross-bridges must be less than 1 (i.e. $\overline{f_{app}}$ cannot be much greater than $\overline{g_{app}}$). This allows an increase in $\overline{f_{app}}$ to increase the number of attached cross-bridges and hence force (Figure 9A). Is this hypothesis reasonable for active lengthening during maximal activation? $\overline{f_{app}}$ during filament sliding is unlikely to be different from $\overline{f_{app}}$ in the isometric condition, because there is no reason to expect the two determinants of $\overline{f_{app}}$, the rate function $f_{app}(\theta)$ and the relative distribution of detached cross-bridges, to be affected by velocity. In contrast, $\overline{g_{app}}$ will most certainly be affected by velocity because the distribution of *attached* cross-bridges is skewed by filament sliding (Figure 8B). During active lengthening the distribution of attached cross-bridges will be skewed to angles greater than the attachment angle, so $\overline{g_{app}}$ during active lengthening should be much larger than $\overline{g_{app}}$ during isometric conditions. It is therefore reasonable to assume that $\overline{f_{app}}$ is not much greater than $\overline{g_{app}}$ during active lengthening. When $\overline{f_{app}}$ is increased due to MRLC phosphorylation or an increase in length, the number of attached cross-bridges then follows this increase in $\overline{f_{app}}$ (Figure 9A). A consequence of our hypothesis, however, is that the fraction of attached cross-bridges must be less during active lengthening than during isometric. This is potentially inconsistent with previous experiments that measured stiffness during active lengthening, which have suggested that there are ca. 15% *more* attached cross-bridges during active lengthening than during isometric (Julian and Morgan, 1979; Lombardi and Piazzesi, 1990). However, these earlier experiments were conducted in frog muscle

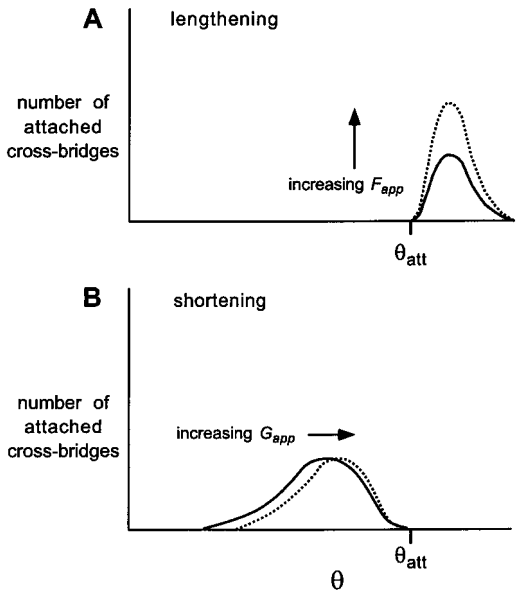

Fig. 9. Effects of increasing cross-bridge attachment/detachment rate constants on the distribution of attached cross-bridges. **A**. Qualitative description of the effects of increasing the rate constant for attachment $\overline{f_{app}}$ during active lengthening. As $\overline{f_{app}}$ increases the number of attached cross-bridges increases, thus increasing net contractile force. Changes in $\overline{f_{app}}$ affect the fraction of attached cross-bridges because during active lengthening $\overline{f_{app}}$ is not much greater than $\overline{g_{app}}$ and so the fraction of attached cross-bridges is much less than 1. **B**. Qualitative description of the effects of increasing the rate constant for detachment $\overline{g_{app}}$ during active shortening. During active shortening $\overline{f_{app}}$ is much greater than $\overline{g_{app}}$, so changes in $\overline{g_{app}}$ will not affect the fraction of attached cross-bridges. Instead, as $\overline{g_{app}}$ increases the relative distribution of attached cross-bridges will shift to larger angles, thus increasing net contractile force.

Table 1. Interactions between potentiation and length

		Effect on sub-maximal, isometric forces[a]	Effect on tetanic, active-lengthening forces[b]	Effect on tetanic, isometric rise times[b]
Effect of potentiation or MRLC phosphorylation	Short lengths	↑↑	↑↑	↑↑
	Intermediate lengths	↑	↑	↑
	Long lengths	0	0[c]	0[c]
Effect of increasing muscle length	Dispot. or MRLC-n	↑	↑	↑
	Pot. or MRLC-P	0	0	0

↑↑, ↑and 0 indicate either a large, moderate or no effect on increasing force or decreasing rise time. Short, intermediate and long lengths refer to 0.8–0.9 L_0, 1.0–1.1 L_0 and 1.3–1.4 L_0 respectively. The dispotentiated and potentiated states are denoted dispot. and pot. while unphosphorylated and phosphorylated MRLC are denoted MRLC-n and MRLC-P.

[a] Yang *et al.* (1998).

[b] Current study.

[c] These results at long lengths were linearly extrapolated from the results at short and intermediate lengths to be zero at ca. 1.4 L_0 (Figures 2 and 4).

at less than 5°C. Coupled with the difference in active lengthening force recorded in these two preparations (ca. 2.0 F_0 in frog vs. 1.4 F_0 in the present experiments), it is possible that there are significant differences between frog at 5°C and cat at 37°C either during active lengthening and/or during isometric conditions.

Active shortening

The effects that we observed during active shortening were significantly different from those observed during active lengthening. For slow to moderate velocities, potentiation had little apparent effect on force at either long or short lengths (similar to previous observations by Persechini *et al.*, 1985; Stuart *et al.*, 1988; Grange *et al.*, 1995). These results are analogous to those seen previously in maximally activated skinned fibers in the isometric state by Sweeney and Stull (1990). In that state, changes in $\overline{f_{app}}$ due to MRLC phosphorylation would have little effect on the fraction of attached cross-bridges because $\overline{f_{app}}$ is much greater than $\overline{g_{app}}$. Is it plausible that $\overline{f_{app}}$ is also much greater than $\overline{g_{app}}$ during active shortening? As the distribution of attached cross-bridges skews to lower values of θ with increasing shortening velocity, $\overline{g_{app}}$ increases. As described above, however, the rate function $g_{app}(\theta)$ increases only slowly as θ decreases from the attachment angle, so the value of $\overline{g_{app}}$ at a given shortening velocity will be approximately one-fifth of the value of $\overline{g_{app}}$ at the corresponding lengthening velocity, making it plausible that $\overline{f_{app}}$ is, in fact, much greater than $\overline{g_{app}}$, at least for moderate shortening velocities.

Our hypothesis makes the prediction that the fraction of attached cross-bridges during moderate speeds of shortening must be high (i.e. close to 100%), similar to the levels during isometric contractions. Early experiments measuring stiffness at maximum shortening velocity suggested that the fraction of attached cross-bridges is ca. 0.2 under conditions of maximal activation (Brenner, 1983; rabbit, 5°C). More recent experiments at higher temperatures (Higuchi and Goldman, 1995; rabbit, 20°C) have suggested that the fraction of attached cross-bridges is ca. 0.5 at maximum shortening velocity. Extrapolating to the temperatures used in the current experiments (37°C) puts the fraction at ca. 0.8. At moderate shortening speeds, which have a correspondingly smaller $\overline{g_{app}}$ than at maximum shortening velocity, the fraction of attached cross-bridges would then be greater than 0.8, consistent with our hypothesis. In such a system, the reduction in contractile force with increased velocity of shortening comes primarily from the change in angular distribution of attached cross-bridges and the reduced contractile force associated with those reduced angles, as opposed to a reduction in the fraction of attached cross-bridges.

We saw a significant effect of length during active shortening regardless of the state of potentiation. At shorter lengths CF produced relatively greater forces during active shortening than at longer lengths. Following the above argument regarding MRLC phosphorylation, we can eliminate changes in $\overline{f_{app}}$ as a potential mechanism. Knowing also that length has no apparent effect on cross-bridge force we are left with the hypothesis that changes in $\overline{g_{app}}$ (and hence $g_{app}[\theta]$) must be responsible for our findings. Because $\overline{f_{app}}$ is much greater than $\overline{g_{app}}$ during active shortening, changes in $\overline{g_{app}}$ will not affect the fraction of attached cross-bridges. If $g_{app}(\theta)$ increases, however, then the mean angle of detachment will be larger, skewing the distribution of attached cross-bridges to larger angles θ (Figure 9B) which correspond to greater cross-bridge forces. Thus an increase in $g_{app}(\theta)$ can lead to greater net contractile force during active shortening through a change in the distribution of attached cross-bridges and not through a change in the fraction of attached cross-bridges. Although speculative, one can imagine that at shorter lengths the increased interfilament spacing would produce a greater tendency for the myosin rod to pull the cross-bridge off the thin filament, thus increasing $g_{app}(\theta)$ and skewing the distribution of attached cross-bridges as described above. An obvious prediction that arises from this hypothesis is that the ATP hydrolysis rate should be higher at shorter lengths due to the associated increase in $\overline{g_{app}}$ (ATPase rate per half-sarcomere is proportional to $\overline{g_{app}}$; Sweeney and Stull, 1990). This prediction has yet to be tested. Because $\overline{g_{app}}$ during active lengthening is significantly greater than $\overline{g_{app}}$ during active shortening, the relative effects of a length-dependent change in $g_{app}(\theta)$ will be much less during active lengthening, perhaps explaining why we did not observe a similar effect of length during those conditions.

Our suggestion that length affects $\overline{g_{app}}$ is consistent with some of our other observations described below, but not with the findings of Yang *et al.* (1998). They showed that length had no effect on the force-pCa relationship of single rabbit fibers in which MRLC had previously been phosphorylated, implying that length does not affect $\overline{g_{app}}$. One plausible explanation for this discrepancy is the large temperature difference in the two preparations (23°C vs. 37°C). Stephenson and Williams (1985: skinned rat fibers) showed that increases in temperature shift the force-pCa relationship to higher concentrations of calcium (through a decrease in $\overline{f_{app}}$ and/or an increase in $\overline{g_{app}}$). Moore *et al.* (1990: intact mouse muscle) showed that increases in temperature decrease twitch relaxation time and increase maximum shortening velocity, both of which are consistent with an increase in $\overline{g_{app}}$. Because $\overline{g_{app}}$ appears to be affected strongly by temperature in these studies, it is plausible that our proposed $\overline{g_{app}}$ length dependence might also be affected by temperature. Alternatively there may be a species-related difference to this phenomenon (rabbit vs. cat).

Slow-twitch FV relationships

The tetanic FV relationship for the 100% slow-twitch feline soleus muscle, which does not potentiate, provides an interesting comparison with CF. In contrast to CF,

soleus's maximum shortening velocity is relatively small and its FV relationship has no apparent length dependence for shortening velocities. Soleus has a strong length dependence for lengthening velocities, producing greater forces during active lengthening at longer lengths (Figure 10; replotted from Scott *et al.*, 1996). The effects of length on active-lengthening force that Scott *et al.* observed in soleus are analogous to those that we observed in dispotentiated CF, and so are easily understood in terms of length-dependent changes in $\overline{f_{app}}$ described above for dispotentiated fast-twitch muscle. Maximum shortening velocity is determined largely by the rate function $g_{app}(\theta)$ and the relationship between cross-bridge force and cross-bridge angle θ. Fiber-type differences in cross-bridge force as a function of θ are relatively small (Malamud *et al.*, 1996) implying that slow myosin has a smaller $g_{app}(\theta)$ than fast myosin. In order to account for the length independence of the shortening FV properties of soleus, we must hypothesize that slow myosin has a $g_{app}(\theta)$ that is relatively independent of myofilament spacing.

Rise and fall times

In these experiments, length and potentiation were observed to have interactive effects on tetanic rise and fall times. These effects can be explained as logical corollaries of our central hypotheses regarding the effects of both sarcomere length and MRLC phosphorylation on $\overline{f_{app}}$ and $\overline{g_{app}}$. During tetanic stimulation of a whole-muscle, initial rise time (t_{0-50}) should be dominated primarily by the effects of cross-bridge attachment because there are no attached cross-bridges to detach. In contrast, later rise time (t_{20-80}) should also be affected somewhat by the detachment of early-formed cross-bridges. During the latter stages of relaxation when very few new cross-bridges are being formed (t_{80-20}), fall time should be dominated primarily by the effects of cross-bridge detachment. In contrast early fall time (t_{100-50}) should also be affected somewhat by the attachment of new cross-bridges. This explains why rise and fall times cannot be characterized by single time-constants and led us to look at these epochs separately.

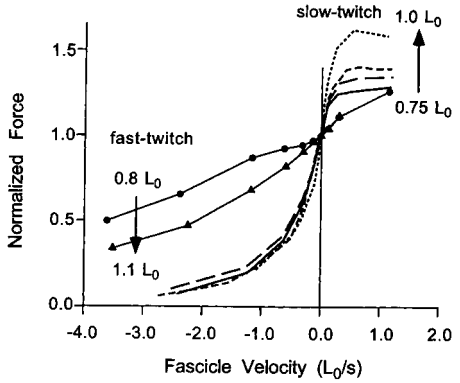

Fig. 10. Effect of length on slow-twitch tetanic FV data. Slow-twitch data were replotted from Figure 6 of Scott *et al.* (1996). Data were collected from five feline soleus muscles using similar methods to those described in the present study, with representative data from one of the animals shown here. Mean fast-twitch data is replotted from Figure 2D. FV data were normalized to isometric forces. In slow-twitch muscle, length had little effect on the shortening half of the FV relationship, but had a large effect on the lengthening half: larger forces were produced at progressively longer lengths. This is in contrast to fast-twitch muscle in which length has a large effect on the shortening half of the FV relationship but no apparent effect on the lengthening half.

Previous experiments in a skinned fiber preparation have shown that MRLC phosphorylation leads to an increase in the rate of force rise (Sweeney *et al.*, 1993) and a decrease in the rate of force relaxation (Patel *et al.*, 1998). Knowing that MRLC phosphorylation has no apparent effect on the rate of detachment $\overline{g_{app}}$ (Sweeney and Stull, 1990), we interpret both of these results in terms of an increase in the rate of cross-bridge attachment $\overline{f_{app}}$ which results in an increase in the *net* cross-bridge attachment rate during force development and a decrease in the *net* cross-bridge detachment rate during relaxation. Although calcium transients obviously play a major role in both rise and fall times, previous evidence from mouse has suggested that length does not affect tetanic calcium transients (Balnave and Allen, 1996). Therefore we have tried to interpret all length dependent effects observed in this study as changes in either $\overline{f_{app}}$ or $\overline{g_{app}}$.

A summary of the interactions between length and potentiation as they affected initial tetanic rise time (t_{0-50}; Figure 4A) is listed in Table 1. The effects of these interactions mirror those discussed previously in relation to tetanic active-lengthening forces and sub-maximal isometric forces, consistent with our hypothesis that changes in $\overline{f_{app}}$ are responsible for the observed effects on initial tetanic rise time. The effects of PAP on t_{20-80} were similar to those on t_{0-50} (implying that $\overline{f_{app}}$ was primarily responsible) whereas the effects of length were somewhat diminished, possibly because of simultaneous changes in $\overline{g_{app}}$. Early fall times (t_{100-50}; Figure 4C) were increased during PAP as expected with an increased $\overline{f_{app}}$, but this increase was length-independent, also possibly because of simultaneous changes in $\overline{g_{app}}$. In contrast, later tetanic fall times (t_{80-20}; Figure 4D) were affected little by potentiation and increased with length regardless of potentiation. This finding is consistent with our above hypothesis that increases in length tend to decrease $\overline{g_{app}}$, hence increasing fall time.

The effects of potentiation on twitch rise and fall times were quite different and largely opposite to the effects on tetanic rise and fall times. Twitch fall time was correlated linearly with length when CF was potentiated and correlated parabolically with length when dispotentiated (Figure 6). In contrast, twitch rise time increased linearly with length in either state and was affected little by potentiation. Many previous studies have examined the effects of either length (Woittiez *et al.*, 1984: dispotentiated rat muscle; Hartree and Hill, 1921; Close, 1972: dispotentiated frog muscle) or activation history (Botterman *et al.*, 1986: cat muscle at L_0; Close and Hoh, 1968; Vandenboom and Houston, 1996: rat and mouse muscle at $> 1.2\ L_0$) on isometric twitch rise and fall times and observed qualitatively similar results to ours.

The different effects of potentiation on twitch dynamics as compared to tetanic dynamics are not readily explainable via the changes in $\overline{f_{app}}$ and $\overline{g_{app}}$ outlined above, suggesting that there is another activation-dependent mechanism occurring in parallel with MRLC phosphorylation. Such an independent mechanism would be likely to have different time constants associated with its development and decay from those associated with MRLC phosphorylation. Figure 7 illustrates the independence in the decay of two phenomena which we believe to be associated with these independent mechanisms. We suggest that the changes in twitch fall time might reflect changes in calcium uptake which are known to be dependent upon many factors (Haynes and Mandveno, 1987; Fink and Veigel, 1996). Although steady-state sarcoplasmic calcium concentrations appear not to be affected by length (Balnave and Allen, 1996), there is no evidence yet to determine if there is an effect of activation history on calcium levels or calcium transients. Previous speculation has suggested that changes in calcium release/uptake might play a role in producing PAP by prolonging the twitch active state; our results show clearly, however, that recent activation shortens the duration of the twitch active state in such a way as to effectively reduce PAP, not to increase it.

Although the effects of PAP on twitch fall time are not readily explainable via changes in $\overline{f_{app}}$ and $\overline{g_{app}}$, we can explain the effects of length on twitch fall time for the potentiated state. As was the case with tetanic fall times, twitch fall times should be dominated by $\overline{g_{app}}$. We have hypothesized above that $\overline{g_{app}}$ decreases with increasing sarcomere length, which should in turn increase twitch fall times, consistent with our observations in Figure 6C and 6D.

Statement of testable hypotheses

The data we have presented here corroborate evidence from many previous studies, insofar as comparisons to data collected at unphysiological colder temperatures can be made. Our interpretation of our data led us to several specific hypotheses that apply to maximally activated mammalian muscle at normal body temperature.

1. The fraction of attached cross-bridges during active lengthening is less than during isometric conditions.
2. The fraction of attached cross-bridges during moderate active shortening is similar to during isometric conditions.
3. Changes in interfilament spacing in a fast-twitch muscle affect the rate constant for cross-bridge detachment.
4. Changes in interfilament spacing in a slow-twitch muscle do *not* affect the rate constant for cross-bridge detachment (or at least have much less of an effect than in fast-twitch muscle).

Each of these predictions is readily testable. If confirmed, this would provide support for a relatively simple and plausible extension of a Huxley-style mechanism to account for a wide range of complex phenomena that can be observed in whole muscles under physiological conditions.

Acknowledgements

The authors would like to thank Janet Creasy for technical assistance with the experiments, Dr H. Lee Sweeney for suggestions on our experiments and Ms. Tiina L. Liinamaa and Dr Frances J. R. Richmond for comments on our manuscript. This research was funded by the Medical Research Council of Canada.

References

Balnave CD and Allen DG (1996) The effect of muscle length on intracellular calcium and force in single fibres from mouse skeletal muscle. *J Physiol* **492:** 705–713.

Botterman BR, Iwamoto GA and Gonyea WJ (1986) Gradation of isometric tension by different activation rates in motor units of cat flexor carpi radialis muscle. *J Neurophysiol* **56:** 494–506.

Brenner B (1983) Crossbridge attachment during isotonic shortening in single skinned rabbit psoas fibers. *Biophys J* **41:** 33a (abstract).

Brenner B (1988) Effect of Ca^{2+} on cross-bridge turnover kinetics in skinned single rabbit psoas fibers: implications for regulation of muscle contraction. *Proc Natl Acad Sci USA* **85:** 3265–3269.

Brown IE, Satoda T, Richmond FJR and Loeb GE (1998) Feline caudofemoralis muscle. Muscle fiber properties, architecture, and motor innervation. *Exp Brain Res* **121:** 76–91.

Brown IE and Loeb GE (1995) A damaged state in cat caudofemoralis muscle induced by high forces. *Can J Physiol Pharmacol* **73:** Ai (abstract).

Brown IE and Loeb GE (1997) The physiological relevance of potentiation in mammalian fast-twitch skeletal muscle. *Soc Neurosci Abstr* **23:** 1049 (abstract).

Brown IE and Loeb GE (1998) Post-activation potentiation: a clue for simplifying models of muscle dynamics. *Am Zool* **38:** 743–754.

Brown IE and Loeb GE (1999) A reductionist approach to creating and using neuromusculoskeletal models. In: Winters JM and Crago PE (eds.) Biomechanics and Neural Control of Movement. Springer-Verlag, New York.

Burke RE, Rudomin P and Zajac FEI (1976) The effect of activation history on tension production by individual muscle units. *Brain Res* **109:** 515–529.

Civan MM and Podolsky RJ (1966) Contraction kinetics of striated muscle fibres following quick changes in load. *J Physiol* **184:** 511–534.

Close R and Hoh JFY (1968) The after-effects of repetitive stimulation on the isometric twitch contraction of rat fast skeletal muscle. *J Physiol* **197:** 461–477.

Close RI (1972) The relations between sarcomere length and characteristics of isometric twitch contractions of frog sartorius muscle. *J Physiol* **220:** 745–762.

Elliott GF, Lowy J and Worthington CR (1963) An x-ray and light-diffraction study of the filament lattice of striated muscle in the living state and in rigor. *J Mol Biol* **6:** 295–306.

Fink RH and Veigel C (1996) Calcium uptake and release modulated by counter-ion conductances in the sarcoplasmic reticulum of skeletal muscle. [Review] *Acta Physiol Scand* **156:** 387–396.

Godt RE and Maughan DW (1981) Influence of osmotic compression on calcium activation and tension in skinned muscle fibers of the rabbit. *Pflügers Arch* **391:** 334–337.

Goldman YE, McCray JA and Vallette DP (1988) Cross-bridges in rigor fibres of rabbit psoas muscle support negative forces. *J Physiol* **398:** 72P (abstract).

Gordon AM, Huxley AF and Julian FJ (1966) The variation in isometric tension with sarcomere length in vertebral muscle fibres. *J Physiol* **184:** 170–192.

Grange RW, Cory CR, Vandenboom R and Houston ME (1995) Myosin phosphorylation augments force-displacement and force-velocity relationships of mouse fast muscle. *Am J Physiol* **269:** C713–C724.

Hartree W and Hill AV (1921) The nature of the isometric twitch. *J Physiol* **55:** 389–411.

Haynes DH and Mandveno A (1987) Computer modeling of Ca^{2+} pump function of Ca^{2+}-Mg^{2+}-ATPase of sarcoplasmic reticulum. *Physiol Rev* **67:** 244–284.

Higuchi H and Goldman YE (1995) Sliding distance per ATP molecule hydrolyzed by myosin heads during isotonic shortening of skinned muscle fibers. *Biophys J* **69:** 1491–1507.

Hill TL (1974) Theoretical formalism for the sliding filament model of contraction of striated muscle. Part I [Review]. *Prog Biophys Mol Biol* **28:** 267–340.

Houston ME and Grange RW (1990) Myosin phosphorylation, twitch potentiation, and fatigue in human skeletal muscle. *Can J Physiol Pharmacol* **68:** 908–913.

Huxley AF (1957) Muscle structure and theories of contraction. *Prog Biophys Mol Biol* **7:** 255–318.

Huxley AF and Simmons RM (1973) Mechanical transients and the origin of muscular force. *Cold Spring Harbor Symp Quant Biol* **37:** 669–680.

Huxley HE (1953) X-ray analysis and the problem of muscle. *Proc R Soc Lond (Biol)* **141:** 59–62.

Julian FJ and Morgan DL (1979) The effect on tension of non-uniform distribution of length changes applied to frog muscle fibres. *J Physiol* **293:** 379–392.

Julian FJ and Sollins R (1975) Variation of muscle stiffness with force at increasing speeds of shortening. *J Gen Physiol* **66:** 287–302.

Krarup C (1981) Enhancement and diminution of mechanical tension evoked by staircase and by tetanus in rat muscle. *J Physiol* **311:** 355–372.

Levine RJC, Kensler RW, Yang Z, Stull JT and Sweeney HL (1996) Myosin light chain phosphorylation affects the structure of rabbit skeletal muscle thick filaments. *Biophys J* **71:** 898–907.

Lombardi V and Piazzesi G (1990) The contractile response during steady lengthening of stimulated frog muscle fibres. *J Physiol* **431:** 141–171.

Macintosh BR and Gardiner PF (1987) Posttetanic potentiation and skeletal muscle fatigue: interactions with caffeine. *Can J Physiol Pharmacol* **65(2):** 260–268.

Malamud JG, Godt RE and Nichols TR (1996) Relationship between short-range stiffness and yielding in type-identified, chemically skinned muscle fibers from the cat triceps surae muscles. *J Neurophysiol* **76:** 2280–2289.

Martyn DA and Gordon AM (1988) Length and myofilament spacing-dependent changes in calcium sensitivity of skeletal fibres: effects of pH and ionic strength. *J Muscle Res Cell Motil* **9:** 428–445.

Metzger JM, Greaser ML and Moss RL (1989) Variations in cross-bridge attachment rate and tension with phosphorylation of myosin in mammalian skinned skeletal muscle fibers. *J Gen Physiol* **93:** 855–883.

Moisescu DG and Thieleczek R (1979) Sarcomere length effects on the Sr^{2+} and Ca^{2+} activation curves in skinned frog muscle fibres. *Biochim Biophys Acta* **546:** 64–76.

Moore RL, Houston ME, Iwamoto GA and Stull JT (1985) Phosphorylation of rabbit skeletal muscle myosin *in situ*. *J Cell Physiol* **125:** 301–305.

Moore RL, Palmer BM, Williams SL, Tanabe H, Grange RW and Houston ME (1990) Effect of temperature on myosin phosphorylation in mouse skeletal muscle. *Am J Physiol* **259:** C432–C438.

Moore RL and Stull JT (1984) Myosin light chain phosphorylation in fast and slow skeletal muscle *in situ*. *Am J Physiol* **247:** C462–C471.

Morano I, Piazzesi G and Rüegg JC (1988) Myofibrillar calcium sensitivity modulation: influence of light chain phosphorylation and positive inotropic drugs on skinned frog skeletal muscle. *Adv Exp Med Biol* **226:** 129–137.

Moss RL, Swinford A and Greaser ML (1983) Alterations in the Ca^{2+} sensitivity of tension development by single skeletal muscle fibers at stretched lengths. *Biophys J* **43:** 115–119.

Patel JR, Diffee GM, Huang XP and Moss RL (1998) Phosphorylation of myosin regulatory light chain eliminates force-dependent changes in relaxation rates in skeletal muscle. *Biophys J* **74:** 360–368.

Persechini A, Stull JT and Cooke R (1985) The effect of myosin phosphorylation on the contractile properties of skinned rabbit skeletal muscle fibers. *J Biol Chem* **260:** 7951–7954.

Scott SH, Brown IE and Loeb GE (1996) Mechanics of feline soleus: I. Effect of fascicle length and velocity on force output. *J Muscle Res Cell Motil* **17:** 205–218.

Stephenson DG and Wendt IR (1984) Length dependence of changes in sarcoplasmic calcium concentration and myofibrillar calcium sensitivity in striated muscle fibres. *J Muscle Res Cell Motil* **5:** 243–272.

Stephenson DG and Williams DA (1982) Effects of sarcomere length on the force-pCa relation in fast- and slow-twitch skinned muscle fibres from the rat. *J Physiol* **333:** 637–653.

Stephenson DG and Williams DA (1985) Temperature-dependent calcium sensitivity changes in skinned muscle fibres of rat and toad. *J Physiol* **360:** 1–12.

Stienen GJ, Versteeg PG, Papp Z and Elzinga G (1992) Mechanical properties of skinned rabbit psoas and soleus muscle fibres during lengthening: effects of phosphate and Ca^{2+}. *J Physiol* **451:** 503–523.

Stuart DS, Lingley MD, Grange RW and Houston ME (1988) Myosin light chain phosphorylation and contractile performance of human skeletal muscle. *Can J Physiol Pharmacol* **66:** 49–54.

Stull JT, Bowman BF, Gallagher PJ, Herring BP, Hsu LC, Kamm KE, Kubota Y, Leachman SA, Sweeney HL and Tansey MG (1990) Myosin phosphorylation in smooth and skeletal muscles: regulation and function [Review]. *Prog Clin Biol Res* **327:** 107–126.

Sweeney HL, Bowman BF and Stull JT (1993) Myosin light chain phosphorylation in vertebrate striated muscle: regulation and function. *Am J Physiol* **264:** C1085–C1095.

Sweeney HL and Stull JT (1990) Alteration of cross-bridge kinetics by myosin light chain phosphorylation in rabbit skeletal muscle: Implications for regulation of actin-myosin interaction. *Proc Natl Acad Sci USA* **87:** 414–418.

Vandenboom R and Houston ME (1996) Phosphorylation of myosin and twitch potentiation in fatigued skeletal muscle. *Can J Physiol Pharmacol* **74:** 1315–1321.

Woittiez RD, Huijing PA and Rozendal RH (1984) Twitch characteristics in relation to muscle architecture and actual muscle length. *Pflügers Arch* **401:** 374–379.

Yang Z, Stull JT, Levine RJC and Sweeney HL (1998) Changes in interfilament spacing mimic the effects of myosin regulatory light chain phosphorylation in rabbit psoas fibers. *J Struct Biol* **122:** 139–148.